lasers become available. Moreover, the ever-present nonlinearities must be considered in developing such lasers—particularly Raman laser action and two photon absorption processes since they limit the power handling capabilities of materials.

ACKNOWLEDGMENTS

The authors are indebted to R. W. Minck, G. W. Ford, and C. W. Peters for many helpful discussions and to C. M. Savage for help in conducting the experiments.

PHYSICAL REVIEW VOLUME 137, NUMBER 3A 1 FEBRUARY 1965

Surface Effects in the Mixed Superconducting State

P. S. SWARTZ AND H. R. HART, JR.
General Electric Research Laboratory, Schenectady, New York
(Received 26 August 1964)

Measurements of the critical transport current above H_{c1} in a variety of $Pb_{0.95}Tl_{0.05}$ samples reveal that the surface can support a large transport current in the mixed state when the magnetic field vector is aligned with the surface. When a geometry is chosen so that the magnetic field vector can be aligned with a single surface (e.g., a cylinder of triangular cross section), the critical currents of opposite polarities differ by over a factor of 3 when the magnetic field vector is parallel to a surface plane; partial rectification is thus observed. The larger critical current is always in a direction that indicates that magnetic flux crosses out of the surface of a type-II superconductor more easily than into the surface. The "anomalous peak effect" (a maximum in the critical current just below H_{c2}) is observed in annealed samples and is identified with the strength of the Saint-James–de Gennes surface film *below* H_{c2} because of the manner in which it is affected by a thin surface film of copper. The critical-transport-current results suggest that two separate mechanisms contribute to the surface transport current in the mixed state. One of these mechanisms is identified with the Saint-James–de Gennes surface film *below* H_{c2}; the second is tentatively associated with a bulk penetration depth. We measured a mixed-state resistivity and separated the contributions from the surface and the bulk. The bulk mixed-state resistivity is found to be independent of the density of bulk defects.

I. INTRODUCTION

IT has been established that superconductivity in a type-II superconductor can persist above the Abrikosov[1] upper critical field H_{c2} in a thin surface layer.[2–6] The critical field of this surface layer is sensitive to the angle the magnetic field vector makes with the surface. When the magnetic field vector is parallel to the surface being explored, superconductivity persists to $H_{c3}=1.69H_{c2}$.[6] As the magnetic field vector is turned out of the plane of the surface, the critical field is reduced rapidly, becoming equal to H_{c2} at 90°.

A second surface phenomenon has been predicted by Bean and Livingston.[7] They calculate that the surface acts as a barrier to the nucleation of the mixed state at H_{c1}, delaying the entrance into the mixed state until magnetic fields somewhat greater than H_{c1}. The work of DeBlois and DeSorbo[8] and Joseph and Tomasch[9] supports the Bean-Livingston prediction.

In this paper we explore various surface phenomena in the mixed state ($H_{c1}\leq H\leq H_{c2}$) and between H_{c2} and H_{c3}. Our more significant findings are: (1) The surface of a type-II superconductor is capable of carrying significant transport supercurrents in the mixed state when the magnetic field vector is parallel to the plane of the surface. (2) The magnitude of the critical surface transport current is sensitive to the polarities of the transport current and the magnetic field in a manner revealing that in a type-II superconductor magnetic flux crosses the surface more easily from within the sample than from without; partial rectification can occur in a superconductor (see *Note Added in Proof*). (3) The "anomalous peak effect"[10,11] near H_{c2} (sometimes called

[1] A. A. Abrikosov, Phys. Chem. Solids **2**, 199 (1957).
[2] C. F. Hempstead and Y. B. Kim, Phys. Rev. Letters **12**, 145 (1964).
[3] H. R. Hart, Jr. and P. S. Swartz, Phys. Letters **10**, 40 (1964).
[4] G. Bon Mardion, B. B. Goodman, and A. Lacaze, Phys. Letters **8**, 15 (1964).
[5] W. J. Tomasch and A. S. Joseph, Phys. Rev. Letters **12**, 148 (1964); M. Cardona and B. Rosenblum, Phys. Letters **8**, 308 (1964); S. Gygax, J. L. Olsen, and R. H. Kropschot, *ibid.* **8**, 228 (1964); Myron Strongin, Arthur Paskin, Donald G. Schweitzer, O. F. Kammerer, and P. P. Craig, Phys. Rev. Letters **12**, 442 (1964); J. P. Burger, G. Deutscher, E. Guyon, and A. Martinet (unpublished).
[6] D. Saint-James and P. G. de Gennes, Phys. Letters **7**, 306 (1964).
[7] C. P. Bean and J. D. Livingston, Phys. Rev. Letters **12**, 14 (1964).
[8] R. W. DeBlois and W. DeSorbo, Phys. Rev. Letters **12**, 499 (1964).
[9] A. S. Joseph and W. J. Tomasch, Phys. Rev. Letters **12**, 219 (1964).
[10] W. DeSorbo, Rev. Mod. Phys. **36**, 90 (1964); S. H. Autler, E. S. Rosenblum, and K. H. Gooen, Phys. Rev. Letters **9**, 489 (1962); J. F. Schenk, J. S. Willis, and R. W. Shaw, Phys. Letters (unpublished).
[11] T. G. Berlincourt, R. R. Hake, and D. H. Leslie, Phys. Rev. Letters **6**, 671 (1961); J. J. Hauser and R. G. Trenting, Phys. Chem. Solids **24**, 371 (1962); R. R. Hake and D. H. Leslie, J. Appl. Phys. **34**, 270 (1963); R. R. Hake, D. H. Leslie, and C. G. Rhodes, *Proceedings of the Eighth International Conference on Low Temperature Physics* (Butterworths Scientific Publications, Ltd., London, 1963), p. 342.

the "dip effect") exists in an annealed lead-based alloy. Studies using copper plating indicate that in our sample the peak effect is a surface phenomenon, apparently a manifestation below H_{c2} of the Saint-James and de Gennes surface sheath.[6]

II. SAMPLE PREPARATION

All of the experiments reported in this paper have been performed with the solid solution $Pb_{0.95}Tl_{0.05}$, a type-II alloy for which $H_{c1}\approx 350$ Oe [12] and $H_{c2}=1030$ Oe. We found previously[3] that the lead-thallium alloys undergo very sharp superconducting transitions between H_{c2} and H_{c3}; these alloys have a very narrow liquidus-solidus range, suggesting little microsegregation upon cooling from the melt. The experiments reported here have been performed with two geometries; thin ribbons 2 in.$\times$0.250 in.$\times\sim$0.003 in. and a 2-in.-long cylinder with a cross section approximating an isoceles right triangle about 0.120 in. wide across the hypotenuse.

The ribbons were prepared by first rolling the cast ingot to 0.004-in. sheet from which samples were cut. The samples were then cotton swabbed with either acetone or ethylene dichloride to remove organic films which would otherwise cause pits to appear on the surface during polishing. The ribbons were polished to a mirrorlike finish by immersing them for 1–2 min in a vigorously stirred solution of 100 parts glacial acetic acid to 26–30 parts of 30% H_2O_2. Following the polish, the samples were immediately washed in ordinary tap water and dried in a fast flowing gaseous nitrogen stream. (If distilled water is used for the wash, a dull film is left on the surface.) The ribbons were then annealed for one to two weeks (at 320$\pm$2°C) in a vacuum ranging between 10^{-6} and 10^{-7} mm. The ribbon specified as "annealed" in this paper was held at 326–327°C for a few minutes after annealing at 320° for a week. The ribbon was mounted between glass plates and current and voltage leads attached (see Fig. 1). The ribbon sample which we designate in this paper as "unannealed" was mounted and tested after the polishing operation.

The cylinders of triangular cross section were prepared by milling from 0.100-in. rolled sheet. Each surface was then sanded flat by rubbing the faces of the triangle against a piece of crocus cloth (No. 685) glued to a flat surface. The subsequent polish, wash, and anneal were then identical to those for the ribbons. A surface layer about 0.002–0.003 in. thick was removed by the polishing operation.

III. EXPERIMENTAL DETAILS

The mounted samples were placed in a helium Dewar between the pole faces of a 12-in. Varian magnet. Two sample orientations have been used; in the first the long axis of the sample is vertical and in the second, horizontal. In the first case the transport-current direction and the magnetic-field vector are always orthogonal ($\theta=90°$) and the magnetic-field vector is rotated in the plane perpendicular to the current direction (azimuthal angle ϕ is varied). In the case of the ribbon, we define $\phi=0°$ when the magnetic-field vector is parallel to the planar faces of the ribbon. For the cylinder of triangular cross section, we define $\phi=0°$ when the magnetic-field vector is parallel to the widest of the three planes. In the second orientation, in which the axis of the sample is mounted horizontally, the magnetic-field vector is kept in a surface plane (azimuthal angle $\phi=0°$) while the angle θ between the transport current and the magnetic field vector H is varied from 0° to 90°.

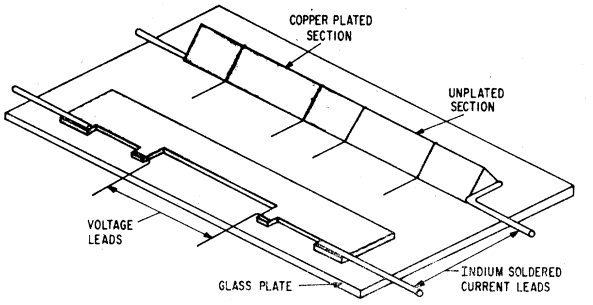

FIG. 1 A schematic of the mounting arrangement of a ribbon and a cylinder of triangular cross section. The glass cover plates are not shown.

The transport current is provided by a Kepco voltage-regulated dc supply and the accompanying voltage drop is measured after amplification by a Liston-Becker dc breaker amplifier. The critical transport current is defined in all experiments as that current at which a voltage drop of 1.4 μV/cm is detected. All experiments were performed at 4.2°K.

IV. SURFACE SUPERCURRENTS; $\theta=90°$ ($I\perp H$), ϕ VARIED

A. Data

In this subsection we report the critical transport current measured as a function of angle ϕ and magnetic field H for ribbons in various conditions and for a well-annealed cylinder of triangular cross section. In the following subsections (B–D) we show that these data provide evidence for surface transport currents in the mixed state.

We determine $\phi=0°$ (H parallel to the plane of the ribbon and, for the cylinder of triangular cross section, to the widest of the three planes) to less than 0.05° by rotating a constant magnetic field of magnitude between H_{c2} and H_{c3} and searching for the voltage minimum. The results for ribbons in three different conditions are displayed in Figs. 2–4. The ribbon of Fig. 2 is in the as-rolled, unannealed condition; that of Fig. 3 is in the annealed condition (one week at 320°C plus a few

[12] J. D. Livingston, Phys. Rev. **129**, 1943 (1963).

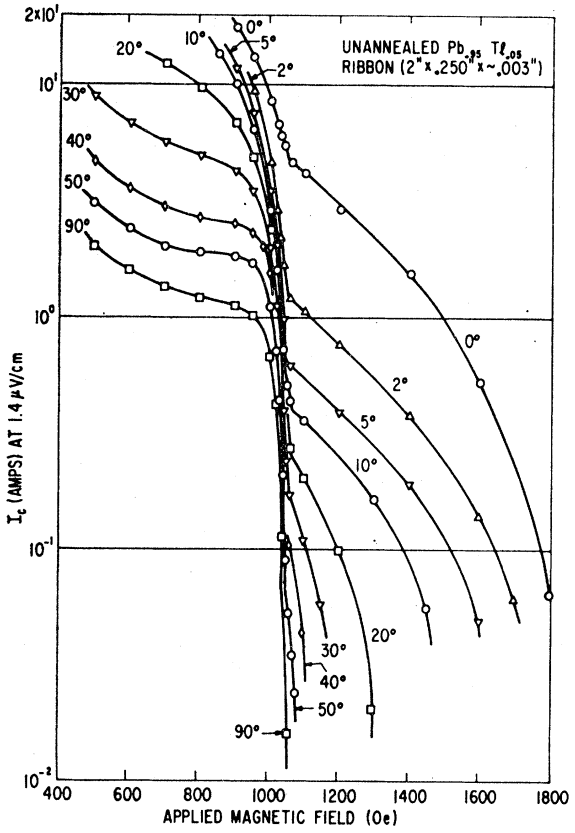

FIG. 2. The experimental family of critical current curves as a function of magnetic field H and azimuthal angle $\phi(H\perp I)$ for an as rolled, unannealed and polished $Pb_{0.95}Tl_{0.05}$ ribbon.

minutes at 326–327°C in vacuo); Fig. 4 shows the ribbon of Fig. 3 after electroplating ~1000 Å of cooper. The following noteworthy features are common to all three families of curves:

1. The critical currents are strongly angular dependent both below and above H_{c2}.
2. At H_{c2} there is a sudden change in the magnitude of the critical current.

The following noteworthy features are not common to all three families of curves:

1. At every angle and field the magnitude of the critical current below H_{c2} is greatest for the unannealed ribbon and least for the copper plated ribbon.
2. Above H_{c2} the magnitude of the critical current is the same for the unannealed and annealed unplated ribbons at all angles except $\phi=0°$.
3. The mangitude of the critical currents above H_{c2} of the annealed plated ribbon is significantly less at all angles than the critical currents of the other two ribbons.
4. At intermediate angles the critical current goes through a maximum just below H_{c2} only on the annealed unplated ribbon. The breadth of these current peaks becomes narrower as the angle ϕ is increased.

The annealed cylinder of triangular cross section was copper-plated over one-half its length[13] (Fig. 1). A pair of voltage leads was attached separately to each half. The critical transport current of the unplated section was determined as a function of azimuthal angle ϕ at $H=700$ Oe (about halfway between H_{c1} and H_{c2}). The results are displayed in Fig. 5. These results have the noteworthy features that:

1. The critical current of each polarity goes through a very sharp maximum when the magnetic field vector is aligned parallel to one of the faces.
2. The magnitude of the critical currents of opposite polarities are significantly different at and near the peaks.
3. The signs of the larger and smaller critical current peaks interchange at each successive surface.
4. The larger and smaller critical currents interchange polarity when the sign of the magnetic field vector is reversed (rotation of 180°).

Below H_{c2} the copper-plated portion of the cylinder demonstrated results essentially the same as those dis-

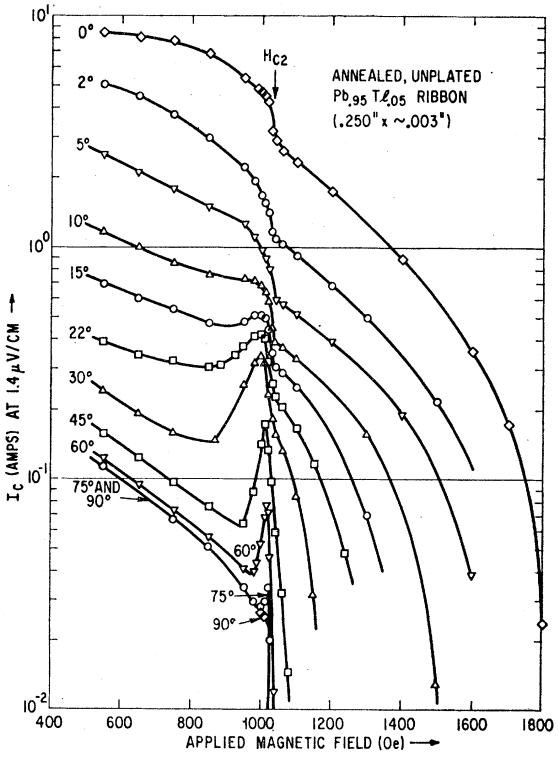

FIG. 3. The experimental family of critical-current curves as a function of magnetic field H and azimuthal angle $\phi(H\perp I)$ for a polished well-annealed ribbon of $Pb_{0.95}Tl_{0.05}$.

[13] The plating of one-half of a specimen in order to study plated and unplated behavior simultaneously was suggested to us by R. W. Shaw.

played in Fig. 5, but with the magnitude of the peaks of each polarity decreased about 50%. In the unplated half of the sample, the critical current went through a maximum as a function of magnetic field just below H_{c2} when the magnetic field vector simultaneously made an angle of at least 30° with each of the three surfaces. No critical current maxima were observed as a function of magnetic field with the copper-plated section.

B. Surface Transport Currents in a Mixed State

In this section we wish to make a single point: the data reveal that surface transport currents flow in the mixed state. The sharp angular dependence of the critical transport current below H_{c2} measured on the unannealed ribbon can tentatively be associated with internal planar defects that originate in the rolling operation. This point has been demonstrated in rolled Nb–Zr and Mo–Re alloys.[11] One would expect that this anisotropy, if associated solely with internal defects, would decrease upon annealing in a single-phase solid solution. We find instead that the anisotropy increases with annealing. In Fig. 6 we display for ribbons in different stages of annealing the critical current as a function of angle at a field of 900 Oe, which is well into the mixed state. With the unannealed ribbon, the critical current drops slightly over an order of magnitude between $\phi=0°$ and $\phi=90°$ (from 17.7 to 1.12 A). The well-annealed ribbon, however, shows a drop of over two orders of magnitude, from 6.1 A at $\phi=0°$ to .043 A at $\phi=90°$. This

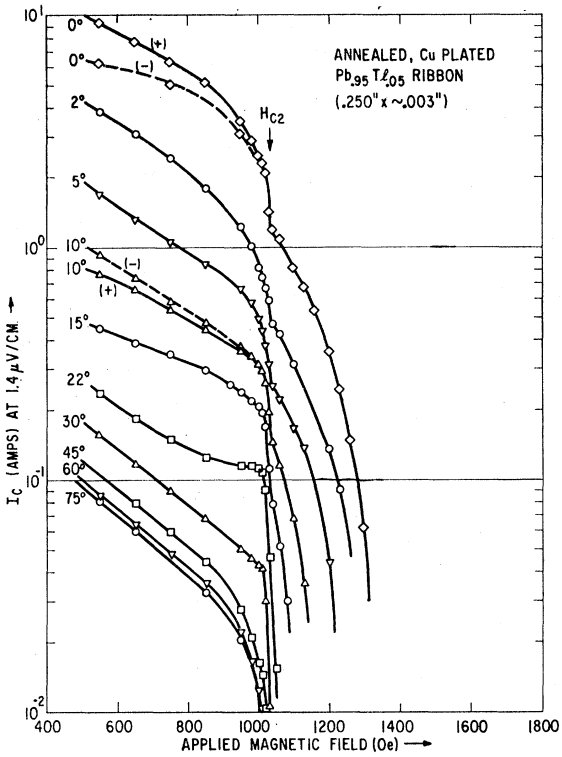

FIG. 4. The experimental family of critical-current curves as a function of magnetic field H and azimuthal angle $\phi(H\perp I)$ for the same ribbon as in Fig. 3 after electroplating ~1000 Å of copper on the surface.

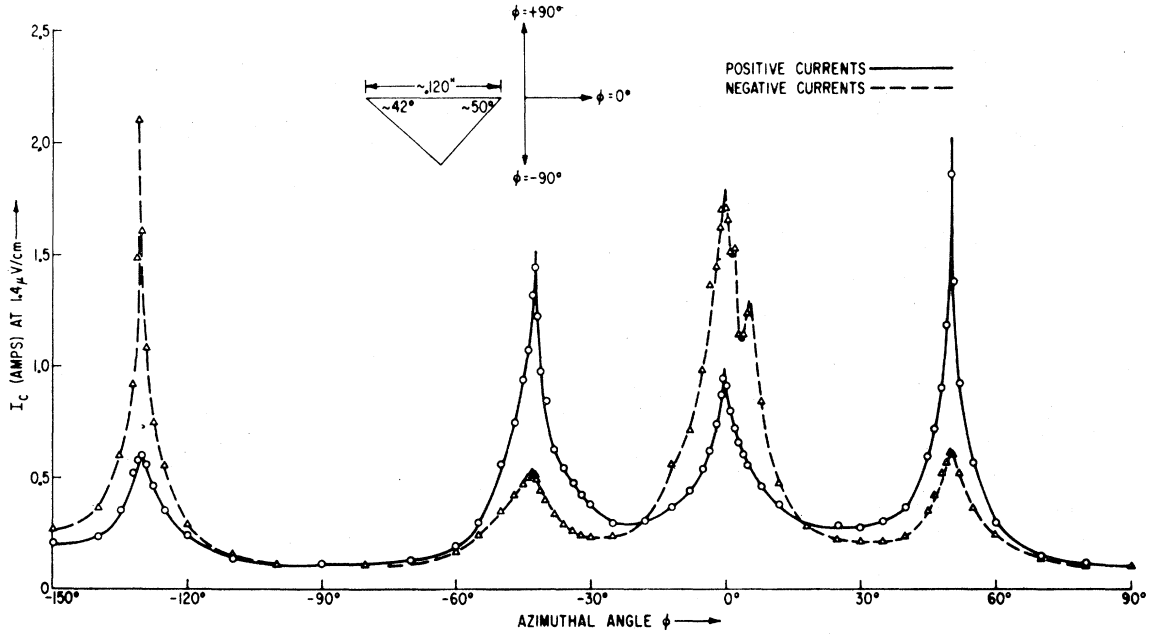

FIG. 5. The critical current of a well-annealed cylinder of triangular cross section as a function of azimuthal angle $\phi(H\perp I)$ at a magnetic field $H=700$ Oe. The results demonstrate that the critical currents of opposite polarities go through maxima of significantly different magnitudes when the magnetic-field vector is aligned parallel to a surface.

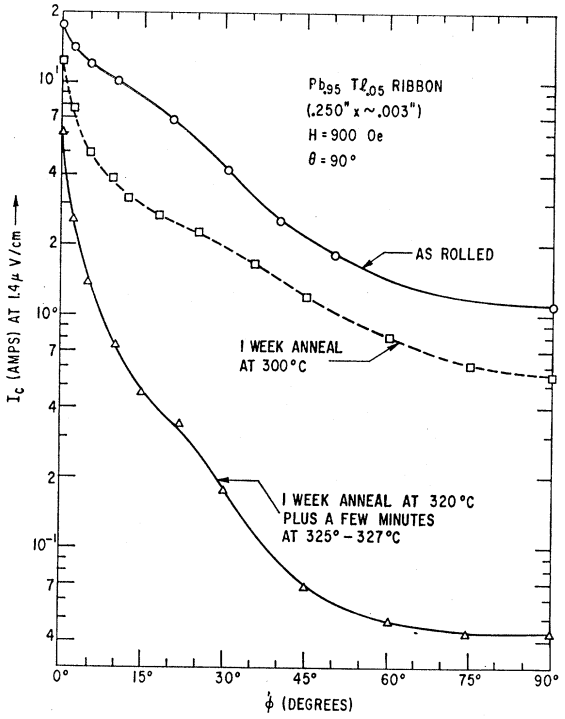

FIG. 6. The angular dependence of critical current for three different ribbons at a magnetic field of 900 Oe and $H \perp I$. The results indicate that the angular dependence of the critical current increases with annealing.

suggests that as the anisotropic bulk currents are removed by annealing, a second mechansim of much sharper angular dependence supports the transport supercurrents. We identify this second mechansim with the surface because of the following observations. When the annealed ribbon which displays the very sharp angular dependence is plated with only about 1000 Å of copper, the critical current is significantly reduced at all fields and angles above H_{c1}. The $\phi=2°$ and $\phi=30°$ curves before and after plating are taken out of Figs. 3 and 4 and displayed separately in Fig. 7. This observation supports a surface mechanism since the strength of any bulk defect should be insensitive to a thin surface layer of copper. The point that surface currents are indeed sensitive to the copper film is demonstrated in Fig. 7 where it may be observed that the critical current is reduced above H_{c2} with copper-plating where only the Saint-James and de Gennes surface currents flow.[2,6]

The argument for transport surface currents in the mixed state is strengthened by the results on the annealed cylinder of triangular cross section. Here the argument cannot be made that the peaks originate from internal rolling planes since only one pair of peaks ($\phi=-42°$) corresponds to a surface parallel to the rolling plane, and yet the three pairs of peaks are generally similar in height and breadth. It is unlikely that planar bulk defects with properties similar to those produced by rolling are introduced by the cutting and sanding operations. In addition, we removed a 0.002-in.–0.003-in. surface layer during the polishing operation prior to the anneal.

One of the more convincing arguments for transport surface currents comes from the partial rectification (i.e., unequal critical currents of opposite polarity) of the applied current at and near each peak (Fig. 5). If rectification were a phenomenon associated with the bulk, then it should appear with equal prominence in the ribbons near $\phi=0°$, but does not. The triangle is distinguished form the ribbon in the essential feature that the magnetic field vector is parallel to only a single surface at a time rather than a pair of surfaces that are mirror images of one another. We interpret the rectification of current applied to the triangles as one of the stronger arguments that the critical transport currents measured in the mixed state with the annealed ribbons and the cylinder of triangular cross section are predominantly surface currents.

C. The Argument for Two Surface Mechanisms in the Mixed State

In this subsection we wish to show that two separate and distinct surface mechanisms contribute to the mixed-state surface currents measured on the two well-annealed ribbons (Figs. 3 and 4) and the annealed cyl-

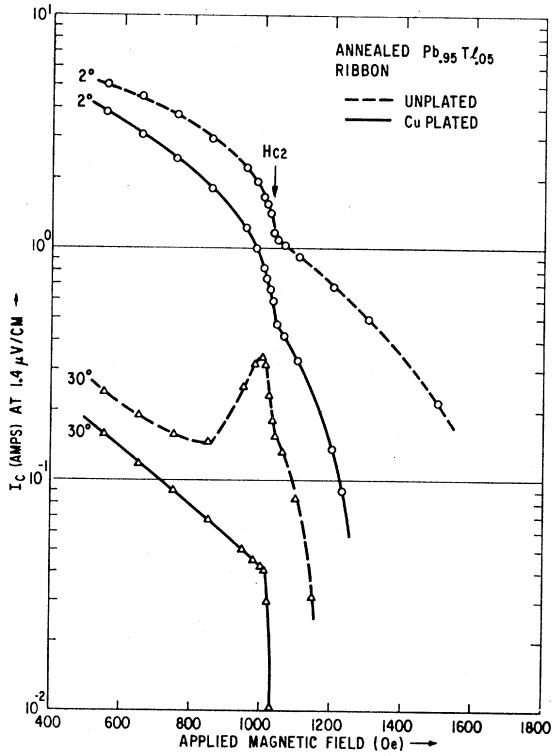

FIG. 7. The critical current as a function of magnetic field at $\phi=2°$ and $\phi=30°$ of a well-annealed ribbon before and after copper electroplating. The curves are taken directly from Figs. 3 and 4 and displayed separately here for easier comparison.

inder of triangular cross section. We arrive at this conclusion from the observation that the family of curves displayed in Figs. 3 and 4 can be constructed from the sum of two families of curves, each having a significantly different field dependence and each affected to a different degree by the copper plating. We display these two families of curves, denoted mechanism A and mechanism B in Figs. 8 and 9. Mechanism A has the assigned property that its contribution to the total mixed-state surface current decreases approximately exponentially with increasing field strength and then cuts off sharply at H_{c2}. We tentatively assign to surface mechanism A an effective surface-layer thickness on the order of the penetration depth λ. Mechanism B has the assigned property that it yields transport supercurrents that are a maximum at or just below H_{c2} and are roughly symmetric about their maximum. For the present discussion this family of curves is constructed by arbitrarily reflecting the critical current curves above H_{c2}, where no contribution from A exists, about a field just below H_{c2}. We identify mechanism B with the Saint-James and de Gennes surface film having an effective thickness on the order of the coherence length ξ. Following this interpretation, the effect of copper will be somewhat more severe on the currents related to a coherence depth than with a penetration depth as $\lambda \gtrsim 2\xi$ in this material.[1]

The "anomalous peaks" which are found at angles

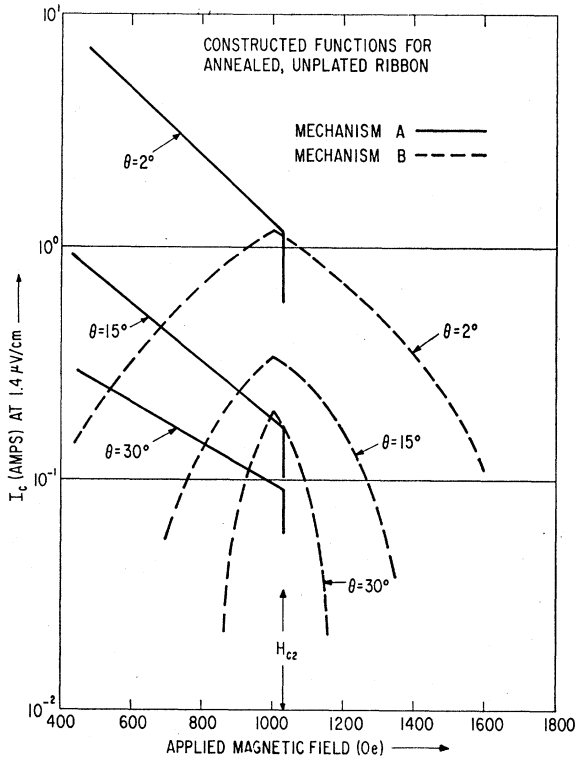

FIG. 8. Two families of constructed critical-current curves for a well-annealed, unplated $Pb_{0.95}Tl_{0.05}$ ribbon. They have the property that when added together they result in a family of curves nearly identical to those of Fig. 3.

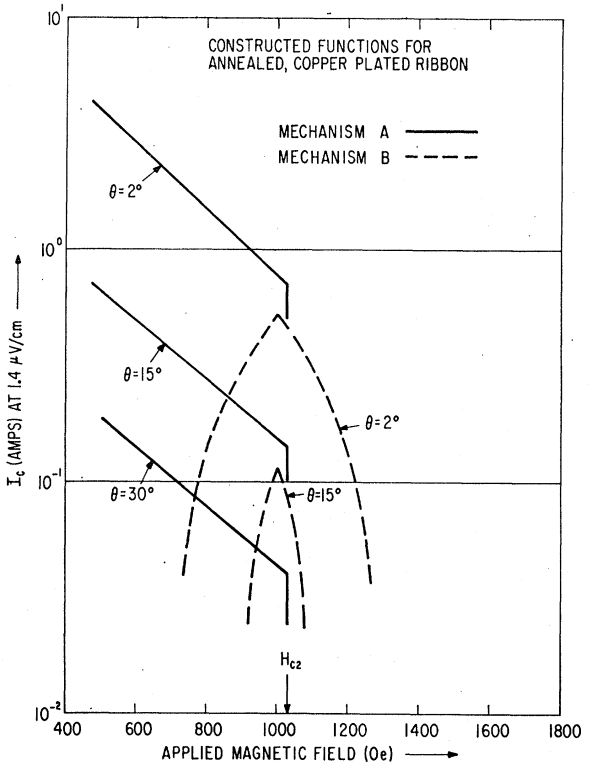

FIG. 9. Two families of constructed critical-current curves for a well-annealed copper-plated $Pb_{0.95}Tl_{0.05}$ ribbon. The dashed curve at $\phi=30°$ falls below the abscissa and is not shown. The curves have the property that when added together they result in a family of curves nearly identical to those of Fig. 4.

intermediate between $\phi=0°$ and $\phi=90°$ in the annealed unplated ribbon and in the unplated portion of the annealed triangle can be explained in terms of these two mechansims. When the magnetic field vector is nearly parallel to a surface, contributions from mechanism A predominate. The currents associated with A show a sharper angular dependence at intermediate angles than those associated with the Saint-James and de Gennes surface sheath. Thus at intermediate angles, the Saint-James and de Gennes mechanism dominates and the current goes through a maximum as a function of magnetic field just below H_{c2}. In this view the current peaks near H_{c2} become sharper as $\phi \rightarrow 90°$ because the critical current curves of the Saint-James and de Gennes surface film above H_{c2} (which are reflected below H_{c2} in mechanism B) drop more sharply with field as $\phi \rightarrow 90°$. At $\phi=90°$ the peaks disappear because the Saint-James and de Gennes surface film does not exist; the critical current here is made up from mechanism A plus perhaps a small remnant contribution from the bulk.

Continuing this interpretation, we can understand the disappearance of the "anomalous peaks" after copper-plating. The copper reduces the magnitude of the cirtical currents above H_{c2} where only the Saint-James and de Gennes mechanism exists by a significantly greater fraction than the critical currents well below

H_{c2} where only mechanism A contributes. When the curves above H_{c2} (Fig. 4) are reflected (Fig. 9) and added to the family of exponential curves, which are determined by the critical current well below H_{c2} in Fig. 4, the peaks do not appear because the exponential curves dominate at all angles. The peaks do not appear for the unannealed ribbon because the bulk currents dominate at all angles (Fig. 2).

With the cylinder of triangular cross section, as with the annealed ribbon, the peaks were observed just below H_{c2} (results not displayed) when the magnetic field vector made an angle of at least 30° with each of the three surfaces. The peaks were not present in the copper-plated section.

The conclusion of the arguments presented in this subsection is that two mechanisms contribute to the surface supercurrents. Mechanism A is undefined in any detail, but may be associated with the bulk penetration depth λ since its contribution to the total surface current cuts off sharply at H_{c2} and since its contribution is less severely affected by copper-plating than is the Saint-James and de Gennes surface film which is associated with a smaller thickness ξ. The "anomalous peaks" below H_{c2} are simply a measure of the strength of the Saint-James and de Gennes surface film below H_{c2}; the peaks are sharpest at angles where the surface currents above H_{c2} fall off most sharply; they disappear with the same copper plating which significantly reduces the strength of the Saint-James and de Gennes surface currents above H_{c2}.

The finding that above H_{c2} identical critical currents were measured for the annealed (Fig. 3) and unannealed (Fig. 2) ribbons for all angles except $\phi=0°$ suggests that these measured surface critical currents ($\phi\neq 0°$) may be fundamental properties of the Saint-James and de Gennes surface film. The annealed sample was polished, then annealed, then tested; the unannealed sample was polished and immediately tested, presumably with a superior surface and thus a higher critical current at $\phi=0°$.

D. The Rectification of Surface Transport Currents

(See *Note Added in Proof.*)

In many of the ribbons tested we measured small differences in the critical currents of each polarity.[14] Typically this difference is 1–2% above H_{c2} and increases to 5–10% near H_{c1}; as $\phi \rightarrow 90°$ the critical currents of each polarity become more nearly equal. In the annealed copper-plated ribbon (Fig. 4) the critical currents of opposite polarity differ by as much as 50% at $\phi=0°$ near H_{c1}, but are essentially the same above H_{c2}. In Fig. 4 the curves shown are those for "positive" current, except at 0° and 10°, where the "negative" critical currents are displayed as well. From 0–2° the positive critical currents are larger; at 2° the positive and negative critical current are about equal; for $\phi>2°$ the negative critical currents are larger; as $\phi \rightarrow 90°$ the critical current becomes independent of polarity.

In the cylinder of triangular cross section the difference between critical currents of opposite polarities becomes significantly more pronounced (Fig. 5). At the peaks the critical currents of opposite polarities differ by about a factor of three. The signs of the larger and smaller current peaks interchange at each successive surface.

In order to understand better these unusual results, let us first note that the critical current is that current for which some small voltage drop is detected (in this paper 1.4 μV/cm). Equivalently,[15] the critical current can be defined as that current which causes a specified amount of magnetic flux to cross the sample per unit time. When the applied magnetic field vector is parallel to a surface carrying a transport supercurrent and perpendicular to the current direction, magnetic flux will cross the surface under the action of the Lorentz force ($\mathbf{I}\times\mathbf{H}$) when the critical-surface transport current (i.e., a critical-surface field gradient) is exceeded. Critical currents of one polarity correspond to magnetic flux crossing the surface from the interior of the sample to the outside; critical currents of the opposite polarity correspond to magnetic flux crossing the surface from the outside in. Similarly, a reversal of magnetic field direction reverses the Lorentz force vector. In terms of this simple treatment it is evident that if magnetic flux can cross a type-II surface more easily in one direction than the other, a single surface will support a larger superconducting transport current in one direction than the other. This model also indicates why the sign of the larger current peak reverses at successive surfaces (Fig. 5) or when the magnetic field vector is rotated 180°; the direction of the Lorentz force reverses in this manner. We find that the larger critical current peaks (Fig. 5) always correspond to a Lorentz force pushing the flux through the surface from without, revealing that it is more difficult for magnetic flux to cross a surface into a type-II superconductor than out of a type-II superconductor. The sharp angular dependence of the critical transport current of each polarity means simply that magnetic flux crosses a surface more easily when the flux crosses at an angle and the Lorentz force direction is not perpendicular to the surface. When the magnetic-field vector makes a large angle with the surface, the flux crosses easily in either direction and the critical currents of each polarity are equal and very small, revealing that the surface is then ineffective as a barrier to the motion of magnetic flux.

In terms of the discussion above one can understand why the critical-transport current measured in type-II ribbons is nearly independent of polarity, even at 0°.

[14] M. A. R. LeBlanc, Rev. Mod. Phys. **36**, 97 (1964).

[15] P. W. Anderson and Y. B. Kim, Rev. Mod. Phys. **36**, 39 (1964); Y. B. Kim, C. F. Hempstead, and A. R. Strnad, Rev. Mod. Phys. **36**, 43 (1964).

When the critical current is reached, magnetic flux crosses both surfaces of the ribbon. One surface is crossed from the outside in, the other from the inside out. As the results from the triangle demonstrate, each surface of the ribbon will support a significantly different transport current when the critical electric field (1.4 μV/cm) is reached. A ribbon with two identical surfaces will not rectify, however, since the reversal of the Lorentz force simply causes the larger and smaller currents to switch to the opposite surfaces while the total current is unchanged. We interpret the small differences between critical transport currents of opposite polarities occasionally observed in ribbons near $\phi=0°$ as caused by a slight difference in the properties of the two surfaces. The larger difference between currents of opposite polarities ($\sim 50\%$) observed in the annealed copper-plated ribbon near H_{c1} and $\phi=0°$ is probably related to a better copper-plating on one surface than the other.

Since there is at present no theory predicting that the surface of a type-II superconductor in the mixed state should act as a barrier to the passage of magnetic flux or that this barrier should be crossed more easily from within that without, it is difficult to say whether the measurements displayed in Fig. 5 and Fig. 10 (the I–V characteristics of the triangle at $H=700$ Oe and $\phi=50°$) are ultimate characteristics or characteristics limited by the quality of the surfaces. Further careful experiments are needed to test this point.

It is possible that the apparent asymmetry of the surface barrier to the crossing of magnetic flux is not a fundamental property of the barrier but is a nucleation phenomenon related to the fact that any quantized flux line lying within a type-II superconductor must break through the surface at some spot. Consider a flux line within the superconductor nearly parallel to a surface and being pushed against the surface barrier by the Lorentz force. The normal spot where the flux line breaks through the surface may weaken the surface barrier locally so that the spot moves down the surface under the influence of the Lorentz force. In this manner the flux line can cross the surface barrier. Magnetic flux being pressed against the surface barrier from without has no such automatic nucleating site available to weaken the barrier locally and permit it to cross. This view of rectification is consistent with the experimental observation that magnetic flux crosses out of a surface more easily than in.

V. SURFACE SUPERCURRENTS: θ VARIED, $\phi=0°$

We have measured the critical current of the annealed copper-plated ribbon as a function of the angle θ between the magnetic-field vector and the transport current, keeping the magnetic-field vector in the plane of the ribbon ($\phi=0°$). Cody, Cullen, and McEvoy[16] have found that Nb_3Sn films obey the Kim-Anderson[15] relationship:

$$J(H\sin\theta+B_0)=\alpha_c,$$

where α_c and B_0 are found to be constants. When we plot I_c^{-1} versus $\sin\theta$ (Fig. 11), we also find a linear relationship and a constant B_0/α_c ratio. The linear relationship between I_c^{-1} and $\sin\theta$ implies that the Lorentz force controls the magnitude of the surface current when the magnetic-field vector is kept in the plane of the surface. The convergence of the straight lines to a single intercept (B_0/α_c) at the ordinate reveals that the strength of the surface superconductivity in the absence of the Lorentz force is a constant, independent of the magnetic field over the field range shown and, for this ribbon, equal to about 40 A, (1/0.026). It is unlikely that this number has fundamental significance. The B_0/α_c ratio is probably a function of surface condition and impurity concentration near the surface. It is also likely that ground planes would further enhance this number by permitting the transport currents to flow more uniformerly over the width of the surface. The calculated α_c is not the same at each magnetic field. A variation of α_c with field is not surprising for this low κ material ($\kappa\simeq 1.36$).[15]

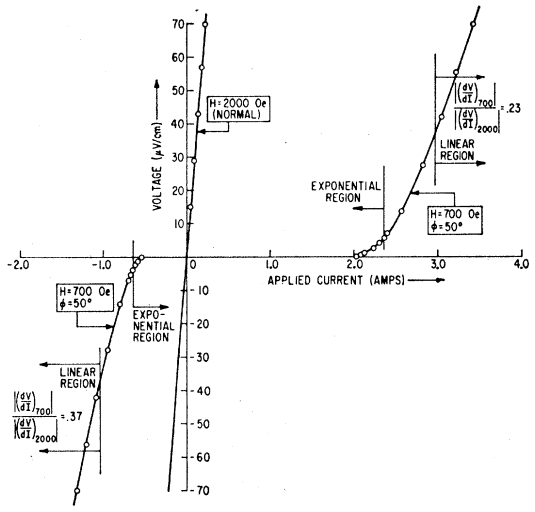

FIG. 10. The voltage versus current transition for the well-annealed cylinder of triangular cross section at $H=700$ Oe and $\phi=+50°$, demonstrating the partial rectification of a superconducting transport current. Initially the voltage increases exponentially with increasing current, but becomes linear in current as the current is further increased.

VI. MIXED-STATE RESISTIVITY

The current-voltage transitions of the ribbons in the three different conditions were also studied. Initially the voltage drop increases exponentially with increasing current ($V/L\sim 5$ μV/cm). Although this exponential region of the transition was not studied in great detail, we developed sufficient data to show that the Kim-

[16] G. D. Cody, G. W. Cullen, and J. P. McEvoy, Jr., Rev. Mod. Phys. **36**, 95 (1964).

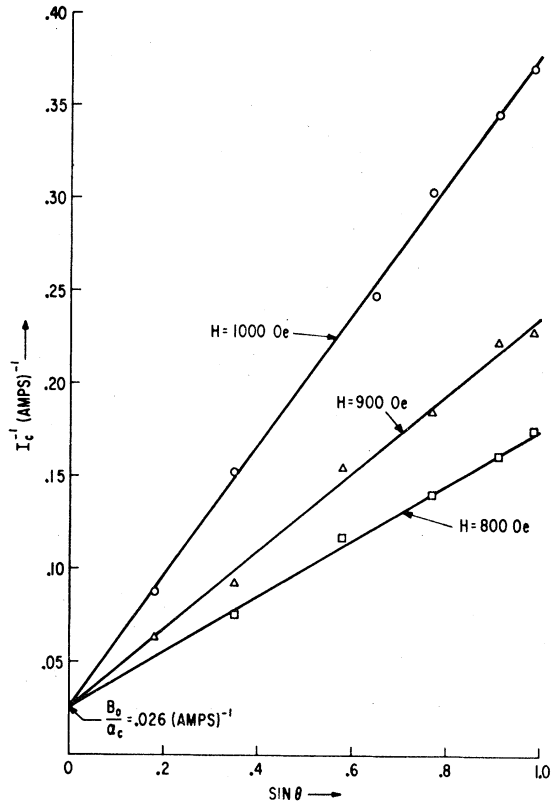

FIG. 11. The inverse of the critical current as a function of the sine of the angle θ between the field and current vectors in the annealed copper-plated ribbon. The magnetic-field vector is kept in the plane of the surface ($\phi=0°$). The linear relationship implies that the critical surface current is controlled by the Lorentz force.

Anderson[15] relationship

$$\ln V=K_1+K_2J(H+B_0)$$

does not hold.

As the voltage drop is increased beyond about 40 μV/cm, the incremental voltage becomes linear with incremental current.[2,17] Figure 10 shows the exponential and linear regions observed in the triangle. The linear region covers an order of magnitude in voltage, beyond which the voltage increases faster than linearly with current, suggesting sample heating.

In the linear region we define a differential resistivity dV/dI; in the mixed state dV/dI is smaller than in the normal state. In Fig. 12 we display for the annealed unplated ribbon the measured differential resistivity divided by the normal-state resistivity (measured at 4.2°K and $H=2000$ Oe) versus applied magnetic field for ϕ equal to 5°, 15°, and 90°. These curves display some interesting features. The resistivity at $\phi=90°$ increases smoothly from zero at a very low magnetic-field strength to the normal-state resistivity at H_{c2}. We associate this resistivity with the bulk rather than the surfaces of the ribbon since at 90° the surfaces support very little supercurrent and are ineffective in impeding the motion of magnetic flux. It is also interesting that the resistivity curve shows no break or change of slope at $H_{c1}(\approx 350$ Oe).[12] This suggests that the sample enters the mixed rather than the intermediate state when flux first penetrates at a low field. (Because of the large demagnetizing factor of the ribbon at $\phi=90°$, magnetic flux will break into the surface at a few Oersteds rather than at H_{c1}.) As the angle ϕ is decreased from 90°, the differential resistivity above H_{c2} becomes less than the normal-state resistivity and the differential resistivity below H_{c2} becomes less than that measured at $\phi=90°$. This suggests that surface superconductivity, being strenghtened by the decreased angle, is able to participate with the bulk in retarding the motion of magnetic flux through the sample. It may be meaningful to calculate a differential resistivity associated with the surface as a function of angle and field by assuming that the lowering of the resistivity with decreasing angle ϕ arises from a low resistivity surface layer or flux barrier in addition to the bulk.

The jog in the resistivity curve at H_{c2} for $\phi\neq 90°$ is not understood. The resistivity curve at $\phi=0°$ could not be determined accurately for the ribbons, because the sample began to heat up soon after the linear region was reached and because the transition became noisy. The scant data we have at 0° indicate that the resistivity is reduced considerably below the curve at $\phi=5°$.

After the annealed ribbon was copper-plated, the resistivity was measured again. The differential resistivity at 90° was unchanged but the resistivity at the other two angles investigated ($\phi=15°$ and $\phi=5°$) showed that the differential resistivity had increased and lay closer to the $\phi=90°$ curve. This is consistent with the interpretation of the data taken prior to plating; the copper film weakens the surface contribution to the resistivity, but has no effect on the bulk properties.

The differential resistivity curve was measured on the unannealed ribbon at $\phi=90°$. This curve was essentially the same as that measured on the annealed sample, though the current at which this linear current-voltage region is found is $\sim$10 times larger. This observation supports the conclusion that beyond a certain critical current the differential resistivity associated with the bulk in the mixed state is insensitive to the defect structure.[2,17]

The angular dependence of the differential resistivity and its interpretation in terms of a combined surface and bulk resistivity suggests that resistivity data taken on round wires may include both a bulk and surface contribution. To minimize the contribution that the surfaces might make to the determination of the bulk resistivity in the mixed state, it may prove desirable to choose a geometry such as a ribbon or film in which the portion of the surface not orthogonal to the flux lines can be made arbitrarily small.

[17] J. Volger, F. A. Staas, and A. G. van Vijfeijken, Phys. Letters 9, 303 (1964); P. H. Borcherds, C. E. Gough, W. F. Vinen, and A. C. Warren (unpublished); W. F. Druyvesteyn and J. Volger, Philips Research Reports (unpublished).

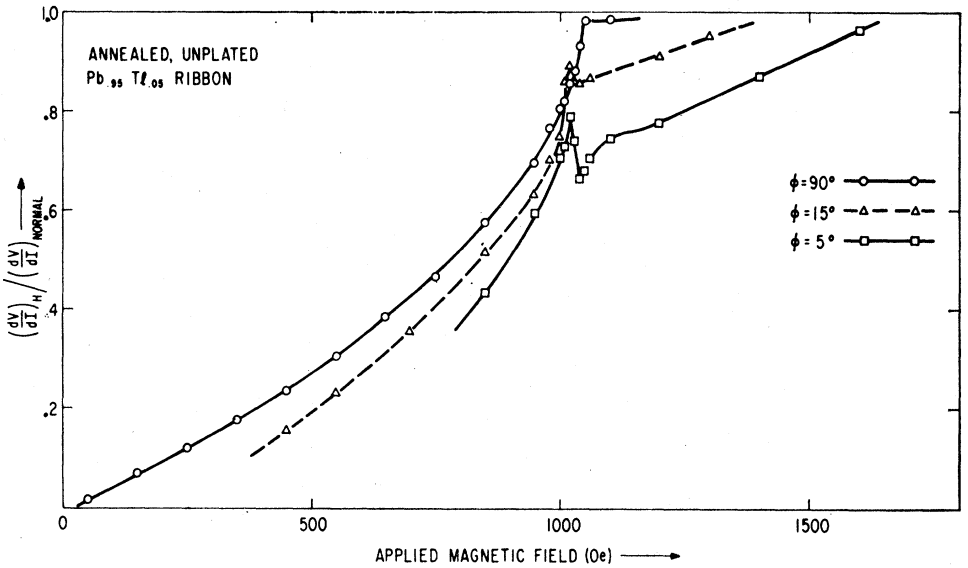

FIG. 12. The normalized differential resistivity of the annealed, unplated $Pb_{0.95}Tl_{0.05}$ ribbon as a function of magnetic field and azimuthal angle ϕ when $H \perp I$. The decrease of resistivity with decreasing angle indicates that the surfaces contribute to the resistivity when ϕ is small.

VII. HALL VOLTAGES

An attempt was made to measure the Hall voltage in the mixed state in the annealed copper-plated ribbon. Voltage probes were placed on opposite edges of the ribbon. The magnetic field vector was directed perpendicular to the major surfaces of the ribbon ($\phi=90°$). This measurement was limited by a spurious effect presumably due to a residual sample imperfection. Upon our reversing the direction of current flow, the small transverse electric field did not simply reverse polarity; there was a change in magnitude as well. This discrepancy (reproducible and magnetic-field-dependent) was on the same order as the change in magnitude of the transverse electric field upon reversing the applied magnetic field. We thus report that in our sample in the mixed state in the linear portion of the I-V curve the transverse or Hall electric field is less than 2% of the longitudinal electric field.[17]

VIII. SUMMARY

The basic conclusion of this work is that the surface of a type-II superconductor is capable of supporting transport supercurrents in the mixed state, as well as above H_{c2}. The magnitude of these currents is extremely sensitive to the angle between the magnetic-field vector and both the surface plane and the current direction. In addition, when the magnetic-field vector is perpendicular to the transport current and nearly parallel to a single isolated surface, rather than a pair of parallel surfaces, the magnitude of the critical transport current of each polarity is significantly different.

The family of curves that describes the total superconducting transport current as a function of angle in unplated and plated annealed ribbons can be related to the sum to two significantly different empirical functions. This leads to the hypothesis that two separate mechanisms contribute to the transport surface current. One of these mechanisms is the Saint-James–de Gennes surface film. It has the postulated property that its strength in supporting transport currents is a maximum at or just below H_{c2} and that its strength, which is strongly angular-dependent, falls off roughly symmetrically on each side of H_{c2} (or a field slightly below H_{c2}). The second surface mechanism is undefined, but characterized by the property that its current carrying capacity decreases approximately exponentially with increasing field beyond H_{c1} and cuts off sharply at H_{c2}. The Bean-Livingston surface barrier may contribute to such a mechanism.

The "anomalous peaks" in the curves of critical current versus magnetic field are observed experimentally in annealed $Pb_{0.95}Tl_{0.05}$ when the magnetic-field vector makes an angle intermediate between $\phi=0°$ and $\phi=90°$; they disappear when copper is plated on the sample, supporting the interpretation that they are of a surface origin in the samples investigated. They apparently result from the field and angular dependence of the Saint-James–de Gennes surface film below H_{c2}.

The absolute magnitude and angular dependence of the critical currents reported for the triangle and the ribbons are probably not a true measure of surface properties. They are certainly sensitive to some degree to surface contamination and surface smoothness. These transport-current curves also probably include a small bulk contribution. The presence of a ground plane should serve to increase the magnitude of the surface transport currents when the mangetic-field vector lies parallel to the surface plane. The transport-current curves measured on the ribbons suffer from an effect revealed by the results of the triangle—when the magnetic field is nearly parallel to the ribbon, the two sur-

faces contribute unequally to the total transport current. Moreover, the larger of the two currents has a much sharper angular dependence. These currents can be separated in the case of the cylinder of triangular cross section. Even here there was no ground plane and the faces of the cylinder could not be made as smooth and planar as those of the ribbon.

A differential resistivity can be measured in the mixed state when the transport current significantly exceeds the critical transport current. This mixed-state resistivity drops sharply from the normal-state resistivity below H_{c2} and approaches zero resistivity at very low magnetic fields. When the magnetic-field vector is perpendicular to the plane of the ribbon and the contribution of the surfaces to the critical current is virtually eliminated, the measured mixed-state resistivity is attributed to the bulk. This resistivity is the same in the annealed and unannealed ribbons and consequently independent of the defect structure. At intermediate angles the surfaces contribute to the superconductivity and the measured differential resistivity is decreased.

In the absence of theories predicting the phenomena we have observed we cannot state the generality of the various effects. It should prove interesting and fruitful to explore these phenomena as a function of surface preparation and contamination, of geometry, and of the Ginzburg-Landau parameter κ.

Note Added in Proof.—Further studies of rectification (to be published) indicate that the mechanism described below is more likely than that described in Sec. IV D. Figures 2–6 show that the surface critical current for a macroscopic sample exhibits a sharp angular peak; any small magnetic field component perpendicular to the surface decreases the critical current. If a sharp angular peak occurs locally for each microscopic region, we can obtain the critical current for the sample by summing the critical currents for the microscopic regions where the local critical currents are determined by the local perpendicular fields $H_\perp(\mathbf{r})$:

$$H_\perp(\mathbf{r})=H_{\perp a}(\mathbf{r})+H_{\perp d}(\mathbf{r})+H_{\perp i}(\mathbf{r}).$$

Here $H_{\perp a}$ is the local perpendicular field applied externally, $H_{\perp d}$ is that resulting from the superconducting diamagnetic currents, and $H_{\perp i}$ is that due to the applied transport current in the sample. If an applied current of one sign gives an $H_{\perp i}(r)$ which tends to cancel the other two terms, a large critical current will be measured, for $H_\perp(r)$ will be small. An applied current of the opposite sign then yields an $H_{\perp i}(r)$ which adds to the other two terms, increasing $H_\perp(r)$ and decreasing the critical current. Rectification can thus occur in a type-II superconductor which has a sharp angular peak in the critical current (it is not necessary that the current be a surface current) and some appropriate local perpendicular field distribution. All rectification experiments performed to date are consistent with this interpretation.

A simple example is a strip having a cross section viewed along the long axis of a circular arc of a large radius of curvature. The applied magnetic field, when parallel to the chord of the arc, yields a perpendicular field component varying linearly with distance across the strip, going through zero and changing sign at the midpoint. Applied currents of one polarity decrease the total perpendicular field, yielding a large critical transport current. With the opposite polarity, the perpendicular components add and a small critical transport current results. Rectification ratios as large as 5:1 have been obtained in this way. The triangular sample reported in this paper apparently rectified because the polishing yielded slightly curved surfaces. It is also possible to rectify with a flat sample and a curved applied field, achieved from separate current-carrying field control wires. Rectification ratios as large as 3:1 have been observed in this manner. In 1962 H. H. Edwards and V. L. Newhouse observed rectification in thin tin films using this technique [J. Appl. Phys. **33**, 868 (1962)].

ACKNOWLEDGMENTS

We gratefully acknowledge helpful conversations with C. P. Bean, J. D. Livingston, and W. DeSorbo and the skillful assistance of T. F. Nealon in performing the experiments.